Bioconjugate Chemistry

Article

pubs.acs.org/bc

Functionalized Two-Photon Absorbing Diketopyrrolopyrrole-Based Fluorophores for Living Cells Fluorescent Microscopy

Hussein Ftouni, Frédéric Bolze,* Hugues de Rocquigny, and Jean-François Nicoud

Laboratoire de Biophotonique et Pharmacologie (UMR 7213), Faculté de Pharmacie, Université de Strasbourg, 74 route du Rhin, CS 60024, 67401 Illkirch, France

ABSTRACT: Two-photon excited microscopy has evolved as a routine technique for long-term cellular and *in vivo* imaging and is now available in most optical microscopy facilities. Classical dyes and fluorescent proteins, developed for epifluorescence or confocal microscopy, are used but unfortunately present a low efficiency upon two-photon excitation inducing the need of high excitation power (over 20 mW). To reduce this excitation power, new dyes need to be developed, allowing really low two-photon excitation power in the milliwatt or sub-milliwatt range. We report here the conception, synthesis, and physicochemical and photophysical properties of new functionalized diketopyrrolopyrrole (DPP) derivatives acting as fluorescent tags for biomolecules. They present high two-photon absorption cross-sections and bright luminescence around 600 nm. These two-photon optimized fluorophores were bioconjugated to HIV-I Tat (44-61), and their cellular localization was observed by two-photon excited microscopy using sub-milliwatt laser excitation power.

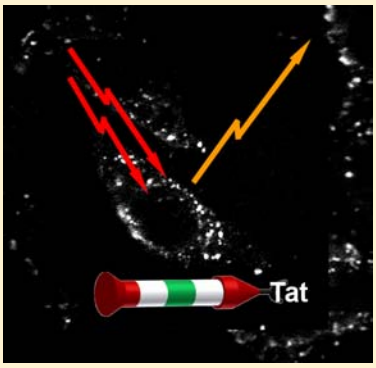

INTRODUCTION

During the past decade, two-photon excited fluorescence (TPEF) imaging methodologies have evolved as powerful techniques for three-dimensional scanning microscopy in biological research, and most microscopy manufacturers propose now commercial TPEF microscopes.[1,2] Indeed, two-photon excitation offers many advantages over conventional confocal microscopy for imaging and for manipulating cellular functions.[3,4] First of all, the two-photon absorption phenomenon occurs at the focal point of the microscope objective, where the laser light intensity is maximum, so that dye bleaching and fluorescence surrounding the focused spot are avoided.[5] In addition, the excitation source is generally an IR laser, which takes advantage of the transparency window of biological tissues and induces reduced phototoxicity compared to that using UV excitation.[6] These combined advantages allow long-term deep imaging *in vivo*.[1] Classical one-photon dyes or fluorescent proteins, well-known in epi-fluorescence or confocal microscopy, are still largely used in two-photon applications, though they exhibit low two-photon absorption cross-sections.[7] Consequently, the development of new dyes or nanostructures (inorganics such as quantum dots,[8] organics such as polymers,[9] or biologics such as viruses[10]), specifically engineered for their two-photon absorption and fluorescence, is of growing emphasis. In addition, the functionalization of such systems to allow conjugation to biologically relevant molecules is crucial for biology.[11,12] Diketopyrrolopyrrole (DPP) derivatives have been known for a long time in the pigment industry due to their bright reddish color, high stability, but also insolubility, which makes them excellent pigments.[13] Recently, we reported the synthesis of molecular water-soluble systemic dyes based on a diketopyrrolopyrrole (DPP) core for TPEF microscopy.[14] These dyes showed good water solubility, efficient two-photon induced fluorescence even in water, and remarkable photostability. We modified these fluorophores in order to allow bioconjugation to an amino group carried by a biomolecule. We report here the synthesis and characterizations of new amino-reactive DPP-based fluorescent probes, their bioconjugation to HIV Trans-Activator of Transcription (Tat) protein chosen as a biomolecule, and the uses of the resulting bioconjugates as two-photon fluorescent probes to image HeLa cells by TPEF microscopy. Two fluorophores based on DPP core will be studied, corresponding formally to a monomer and to a dimer. The bioconjugation in the case of the monomer occurs directly on the DPP central core, and for the dimer it occurs in the periphery of the molecule (Figure 1 left and right, respectively) leading to different geometries for the resulting bioconjugated systems.

Both approaches yielded to fluorophores with high two-photon absorption cross-sections and high fluorescence quantum yields. The Tat (44-61) peptide bioconjugation was efficient, and the resulting bioconjugated probes allowed the

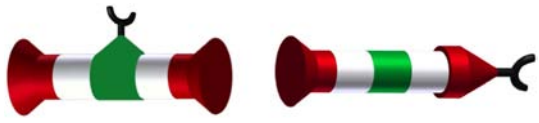

Figure 1. The two architectures of prepared functionalized fluorophores (red, electron-donating group; white, conjugated system; green, DPP central core; and black, reactive function): central (left) and peripheral (right) functionalization.

Received: November 23, 2012
Revised: March 25, 2013
Published: April 12, 2013

dx.doi.org/10.1021/bc300623q | *Bioconjugate Chem.* 2013, 24, 942−950

acquisition of bright two-photon images on HeLa cells with low power excitation.

EXPERIMENTAL SECTION

Materials and Methods. All chemicals and reagents were purchased from Aldrich or Acros Organics and were used as received unless specified. For solid-phase synthesis, 9-fluorenylmethoxycarbonyl (Fmoc) amino acids were supplied by NeoMPS (Strasbourg, France), and resin was from NovaBiochem (Darmstadt, Germany). THF was distilled over sodium and benzophenone under argon atmosphere, dichloromethane was distilled over calcium hydride under argon atmosphere, triethylamine was distilled over potassium hydroxide under argon atmosphere, and DMSO was distilled over calcium hydride under vacuum and conditioned under argon prior to use. ^{1}H and ^{13}C spectra were recorded with a 400 MHz Bruker Advance 400 instrument in $CDCl_3$ (internal standard 7.24 ppm for ^{1}H and 77 ppm, middle of the three peaks, for ^{13}C spectra) or DMSO-d_6 (internal standard 2.26 ppm for ^{1}H and 39.5 ppm for ^{13}C spectra). FAB mass spectra were recorded with a ZA-HF instrument with 4-nitrobenzyl alcohol as a matrix, and ESI spectra were obtained on a Bruker HTC ultra (ESI-IT). TLC analyses were run on Merck precoated aluminum plates (Si 60 F254). Column chromatographies were run on Merck Silica Gel (60−120 mesh). Ethyl 4,5-dihydro-5-oxo-2-phenyl(1*H*)pyrrole-3-carboxylate[15] and 6-bis(4-bromophenyl)pyrrolo[3,4-*c*]-pyrrole-1,4-(2*H*,5*H*)-dione (**6**)[16] were prepared as described previously.

Synthetic Procedures and Characterization. *3-(4-Bromophenyl)-6-phenylpyrrolo[3,4-c]pyrrole-1,4(2H,5H)-dione (**1**).*[16] *tert*-Amyl alcohol (40 mL) and 0.64 g (0.026 mol) of sodium (added in small portions, CAUTION) were mixed and heated to reflux under an argon atmosphere in the presence of catalytic amount of $FeCl_3$, whereupon 4-bromobenzonitrile (2.36 g, 13 mmol, 1 equiv) was added. After that, pyrrolinone ester (3 g, 13 mmol, 1 equiv) dissolved in 30 mL of *tert*-amyl alcohol was introduced dropwise within 15 min. This mixture was stirred under reflux for 2 h. The reaction mixture was then cooled to 60 °C, whereupon acetic acid (10 mL) was added during 10 min. The suspension was heated to 100 °C for 20 min and filtered while remaining hot. The filter cake was washed abundantly with hot ethanol and finally with hot water to give **1** in 70% yield (3.3 g). This material shows similar characteristics as those described in the literature.[13]

*3-(4-Bromophenyl)-2,5-bis(2-(2-methoxyethoxy)ethyl)-6-phenylpyrrolo[3,4-c]pyrrole-1,4(2H,5H)-dione (**2**).* Under an argon atmosphere, **1** (10 g, 27 mmol, 1 equiv) was suspended in *N*-methylpyrrolidinone (150 mL), and potassium *tert*-butoxide (10 g, 89 mmol, 3 equiv) was added fraction wise. The mixture was then heated up to 60 °C, and 1-bromo-2-(2-methoxyethoxy)ethane (15 g, 81 mmol, 3 equiv) was added. Heating and stirring were maintained for 24 h. The mixture was diluted with toluene (200 mL) and filtered. The filtrate was then dried with $MgSO_4$ and evaporated under vacuum. The crude product was purified by column chromatography (silica, CH_2Cl_2/MeOH 98:2 v/v) to give **2** as an orange powder (5.5 g, 36% yield). ^{1}H NMR (400 MHz, $CDCl_3$, 25 °C) δ ppm 7.95−7.93 (m, 2H), 7.9 (d, J = 8.5 Hz, 2H), 7.63 (d, J = 8.5 Hz, 2H), 7.50−7.48 (m, 3H), 3.74−3.96 (m, 4H), 3.53−3.49 (m, 4H), 3.44−3.41(m, 4H), 3.31 (s, 6H), 3.30 (s, 6H). ^{13}C NMR (400 MHz, $CDCl_3$, 25 °C) δ ppm 163.14, 148.00, 132.30, 131.50, 131.15, 129.51, 129.04, 128.14, 127.10, 125.97, 110.07, 72.03, 70.73, 70.67, 69.15, 69.05, 59.25, 53.63, 42.51, 42.217. HRMS m/z calcd for $C_{28}H_{31}BrN_2O_6$ 570.13655, found 570.13724.

*(E)-3-(4-(4-Hydroxy-3,5-dimethoxystyryl)phenyl)-2,5-bis(2-(2-methoxyethoxy)ethyl)-6-phenylpyrrolo[3,4-c]pyrrole-1,4-(2H,5H)-dione (**3**).* Under an argon atmosphere, **2** (500 mg, 0.9 mmol, 1 equiv), palladium acetate (100 mg, 0.45 mmol, 0.5 equiv), and tri(*o*-tolyl)phosphine (160 mg, 0.5 mmol, 0.6 equiv) were suspended in anhydrous DMF (40 mL) and freshly distilled triethylamine (50 mL). The mixture was heated at 50 °C for 1 h, and a solution of 4-(*tert*-butyldimethylsilanyloxy)-3,5-dimethoxystyrene (335 mg, 1.1 mmol, 1.3 equiv) in triethylamine (10 mL) was added. The resulting mixture was heated to 130 °C for 48 h. After cooling the mixture was filtered on Celite, and the solvent was evaporated under vacuum. The solid residue was dissolved in dichloromethane, washed with water, and evaporated under vacuum after being dried over $MgSO_4$. The crude compound was purified by column chromatography (silica, CH_2Cl_2/MeOH 95:5 v/v) to give pure **3** as an orange solid (450 mg, 76% yield). ^{1}H NMR (400 MHz, $CDCl_3$) δ ppm 7.99 (d, J = 8.3 Hz, 2H), 7.94−7.92 (m, 2H), 7.58 (d, J = 8.3 Hz, 2H), 7.49−7.47 (m, 3H), 7.1 (d, J = 16 Hz, 1H), 6.96 (d, J = 16 Hz, 1H), 6.75 (s, 2H), 3.96−3.92 (m, 10H), 3.75−3.69 (m, 4H), 3.54−3.49 (m, 4H), 3.45−3.40 (m, 4H), 3.31 (s, 3H), 3.29 (s, 3 H). ^{13}C NMR (75.75 MHz, $CDCl_3$) δ ppm 163.28, 163.12, 162.70, 149.01, 148.84, 147.47, 140.60, 135.60, 131.26, 129.95, 129.47, 128.96, 128.66, 128.24, 128.22, 126.73, 126.64, 125.99, 109.94, 109.78, 103.92, 72.01, 70.67, 70.63, 69.11, 69.07, 59.22, 56.57, 42.38, 42.16. HRMS m/z calcd for $C_{38}H_{42}N_2O_9$ 670.28903, found 670.28918.

*(E)-tert-Butyl-2-(4-(4-(2,5-bis(2-(2-methoxyethoxy)ethyl)-3,6-dioxo-4-phenyl-2,3,5,6-tetrahydropyrrolo-[3,4-c]pyrrol-1-yl)styryl)-2,6-dimethoxyphenoxy) Acetate (**4**).* Under an argon atmosphere, **3** (300 mg, 0.45 mmol, 1 equiv), methyl chloroacetate (4.97 g, 46 mmol, 1 equiv), and potassium carbonate (310 mg, 2.25 mmol, 5 equiv) were suspended in anhydrous DMF (30 mL) and heated to 90 °C for 5 min. *tert*-Butyl bromoacetate (180 mg, 0.9 mmol, 5 equiv) was then added, and the heating was maintained for 48 h. After cooling, the solvent was evaporated under vacuum, and the crude solid was purified by column chromatography (silica, CH_2Cl_2/MeOH 95:5 v/v) leading to **4** as an orange solid (100 mg, 28% yield). ^{1}H NMR (400 MHz, $CDCl_3$) δ ppm 7.98 (d, J = 8.4 Hz, 2H), 7.93−7.90 (m, 2H), 7.58 (d, J = 8.4 Hz, 2H), 7.47−7.45 (m, 3H), 7.1 (d, J = 16 Hz, 1H), 6.99 (d, J = 16 Hz, 1H), 6.718 (s, 2H), 4.53 (s, 2H), 3.95−3.91 (m, 4H), 3.87 (s, 6H), 3.73−3.68 (m, 4H), 3.52−3.47 (m, 4H), 3.43−3.39 (m, 4H), 3.29 (s, 3H), 3.28 (s, 3 H), 1.44 (s, 9H). ^{13}C NMR (75.75 MHz, $CDCl_3$) δ ppm 168.49, 163.09, 162.96, 162.56, 152.80, 148.78, 140.18, 137.00, 132.46, 131.15, 130.81, 129.81, 129.32, 128.81, 128.48, 128.05, 127.14, 127.05, 126.85, 126.66, 109.77, 109.69, 104.21, 81.53, 71.84, 70.49, 70.46, 70.11, 68.95, 68.90, 59.05, 56.33, 42.21, 42.00, 28.16. HRMS m/z calcd for $C_{44}H_{52}N_2O_{11}$ 784.35711, found 784.35781.

*(E)-2-(4-(4-(2,5-Bis(2-(2-methoxyethoxy)ethyl)-3,6-dioxo-4-phenyl-2,3,5,6-tetrahydropyrrolo[3,4-c]pyrrol-1-yl)styryl)-2,6-dimethoxyphenoxy)acetic Acid (**5**).* Under an argon atmosphere, **4** (95 mg, 0.12 mmol, 1 equiv) was dissolved in dichloromethane (10 mL), and the solution was cooled to 0 °C. Trifluoroacetic acid (3 mL) was added dropwise, and the mixture was stirred at room temperature for 16 h. The solvent was removed under vacuum, and the crude product was purified by column chromatography (silica, CH_2Cl_2/MeOH 90:10 v/v). The desired compound **5** was obtained as an

dx.doi.org/10.1021/bc300623q | *Bioconjugate Chem.* 2013, 24, 942−950

orange solid (85 mg, 97% yield). ^{1}H NMR (400 MHz, $CDCl_3$) δ ppm 7.97−7.89 (m, 4H), 7.58−7.56 (m, 2H), 7.48−7.46 (m, 3H), 7.09 (d, J = 16 Hz, 1H), 7.00 (d, J = 16 Hz, 1H), 6.73 (s, 2H), 4.60 (s, 2H), 3.95−3.89 (m, 10H), 3.71−3.66 (m, 4H), 3.53−3.48 (m, 4H), 3.44−3.41 (m, 4H), 3.3 (s, 6H). ^{13}C NMR (75.75 MHz, $CDCl_3$) δ ppm 171.21, 163.16, 163.10, 152.33, 149.11, 149.11, 139.82, 136.43, 134.15, 131.31, 130.26, 129.97, 129.75, 129.45, 128.95, 128.35, 128.153, 127.33, 126.90, 109.77, 109.88, 103.83, 72.01, 71.60, 70.74, 70.60, 69.05, 59.21, 56.46, 42.22, 42.06. HRMS m/z calcd for $C_{40}H_{44}N_2O_{11}$ 728.29451, found 728.29642.

*3,6-Bis(4-bromophenyl)-2-octylpyrrolo[3,4-c]pyrrole-1,4-(2H,5H)-dione (**7**).* Using the same procedure as for **2**, the desired compound **7** was obtained (300 mg, 15% yield) starting from **6** (1.6 g, 3.6 mmol, 1 equiv), potassium *tert*-butoxide (0.4 g, 3.6 mmol, 1 equiv), NMP (80 mL), and 1-bromooctane (0.7 g, 3.6 mmol, 1 equiv). ^{1}H NMR (400 MHz, $CDCl_3$) δ ppm 9.97 (s, 1H), 8.14 (d, J = 8.6 Hz, 2H), 7.66 (d, J = 8.7 Hz, 2H), 7.63 (d, J = 8.7 Hz, 2H), 7.55 (d, J = 8.6 Hz, 2H), 3.76 (t, J = 7.6 Hz, 2H), 1.26−1.20 (m, 12H), 0.84 (t, J = 7.00 Hz, 3H). HRMS m/z calculated for $C_{26}H_{26}Br_2N_2O_2$ 556.03610, found 556.03644.

*tert-Butyl-2-(3,6-bis(4-bromophenyl)-5-octyl-1,4-dioxo-4,5-dihydropyrrolo[3,4-c]pyrrol-2(1H)-yl) Acetate (**8**).* Using the same procedure as for **2**, the desired compound **8** was obtained (170 mg, 47% yield) starting from **7** (300 mg, 0.54 mmol, 1 equiv), potassium *tert*-butoxide (110 mg, 0.98 mmol, 1 equiv), NMP (30 mL), and *tert*-butyl bromoacetate (160 mg, 0.82 mmol, 1 equiv). ^{1}H NMR (400 MHz, $CDCl_3$) δ ppm 7.57−7.52 (m, 8H), 4.33 (s, 2H), 3.67 (t, J = 7.6 Hz, 2H), 1.47−1.43 (m, 2H), 1.3 (s, 9H), 1.23−1.14 (m, 10H), 0.81 (t, J = 7.00 Hz, 3H). ^{13}C NMR (75.75 MHz, $CDCl_3$) δ ppm 167.48, 162.54, 161.92, 148.225, 146.83, 132.26, 130.29, 130.17, 126.89, 126.78, 126.09, 126.02, 110.58, 109.20, 82.91, 43.89, 41.87, 31.85, 29.39, 29.20, 29.09, 28.15, 27.97, 26.79, 22.74, 14.22. HRMS m/z calcd for $C_{26}H_{26}Br_2N_2O_2$ m/z 556.03610, found 556.03644.

*tert-Butyl-2-(3,6-bis(4-((E)-4-methoxystyryl)phenyl)-5-octyl-1,4-dioxo-4,5-dihydropyrrolo[3,4-c]pyrrol-2(1H)-yl) Acetate (**9**).* Using the same procedure as for **3**, the desired compound **9** was obtained as a red powder (170 mg, 86% yield) starting from **8** (170 mg, 0.25 mmol, 1 equiv), palladium(II) acetate (5.7 mg, 0.025 mmol, 0.10 equiv), tri(*o*-tolyl)phosphine (23.1 mg, 0.076 mmol, 0.30 equiv), anhydrous DMF (8 mL), freshly distilled triethylamine (15 mL), and 4-vinylanisole (85 mg, 0.634 mmol, 2.5 equiv). ^{1}H NMR (400 MHz, $CDCl_3$) δ ppm 7.79 (d, J = 8.2 Hz, 2H), 7.76 (d, J = 8.2 Hz, 2H), 7.57−7.53 (m, 4H), 7.45−7.42 (m, 4H), 7.15 (d, J = 16 Hz, 1H), 7.14 (d, J = 16 Hz, 1H), 6.97 (d, J = 16 Hz, 1H), 6.96 (d, J = 16 Hz, 1H), 6.88 (d, J = 8 Hz, 4H), 4.45 (s, 2H), 3.81 (s, 6H), 3.78 (t, J = 8 Hz, 2H), 1.64−1.56 (m, 2H), 1.35 (s, 9H), 1.26−1.19 (m, 10H), 0.83 (t, J = 7,0 Hz, 3H). ^{13}C NMR (75.75 MHz, $CDCl_3$) δ ppm 167.87, 163.06, 162.42, 159.96, 148.67, 147.19, 140.77, 130.69, 130.66, 129.84, 129.81, 129.39, 129.25, 128.93, 128.29, 126.81, 126.72, 126.65, 125.73, 125.69, 125.64, 114.43, 113.89, 110.64, 109.20, 82.69, 55.52, 53.61, 44.48, 42.31, 31.93, 29.59, 29.31, 29.22, 29.13, 28.08, 26.95, 22.80, 14.26. HRMS m/z calcd for $C_{50}H_{54}N_2O_6$ 778.3982, found 778.3975.

*2-(3,6-Bis(4-((E)-4-methoxystyryl)phenyl)-5-octyl-1,4-dioxo-4,5-dihydropyrrolo[3,4-c]pyrrol-2(1H)-yl)acetic Acid (**10**).* Using the same procedure as for **5**, the desired compound **10** was obtained as a red powder (130 mg, 85% yield) starting from **9** (170 mg, 0.218 mmol, 1 equiv), CH_2Cl_2 (12 mL), and trifluoroacetic acid (6 mL, 78 mmol). ^{1}H NMR (400 MHz, $CDCl_3$) δ ppm 7.82−7.76 (m, 4H), 7.2−7.59 (m, 4H), 7.47−7.44 (m, 4H), 7.20−7.13 (m, 2H), 7.01−7.95 (m, 2H), 6.91−6.87 (m, 4H), 4.54 (s, 2H), 3.82−3.72 (m, 8H), 1.66−1.57 (m, 2H), 1.24−1.19 (m, 10H), 0.83 (t, J = 6.5 Hz, 3H). ^{13}C NMR (75.75 MHz, $CDCl_3$) δ ppm 207.26, 170.92, 163.16, 163.10, 163.07, 163.04, 160.05, 150.16, 146.50, 141.312, 141.24, 131.13, 131.09, 129.79, 129.82, 129.41, 128.99, 128.40, 127.04, 126.82, 126.49, 125.91, 125.60, 114.48, 111.00, 108.64, 55.59, 44.62, 44.55, 32.53, 31.95, 31.14, 29.65, 29.33, 29.23, 26.97, 22.82, 14.29. HRMS m/z calcd for $C_{46}H_{46}N_2O_6$ 722.3356, found 722.3412.

*(2,5-Bis(2-(2-methoxyethoxy)ethyl)-3,6-bis(4-((E)-4-methoxystyryl)phenyl)pyrrolo[3,4-c]pyrrole-1,4(2H,5H)-dione (**11**).* Using the same procedure as for **3**, the desired compound **11** was obtained as a red powder (82 mg, 70% yield) starting from (2,5-bis(2-(2-methoxyethoxy)ethyl)-3,6-bis-(4-bromophenyl) pyrrolo[3,4-*c*]pyrrole-1,4(2*H*,5*H*)-dione[14] (100 mg, 0.154 mmol, 1 equiv), palladium(II) acetate (3.5 mg, 0.0154 mmol, 0.10 equiv), tri(*o*-tolyl)phosphine (14.1 mg, 0.0452 mmol, 0.30 equiv), anhydrous DMF (8 mL), freshly distilled triethylamine (15 mL), and 4-vinylanisole (62 mg, 0.462 mmol, 2.5 equiv). ^{1}H NMR (400 MHz, $CDCl_3$) δ ppm 8.00 (d, J = 8.3 Hz, 4H), 7.60 (d, J = 8.3 Hz, 4H), 7.48 (d, J = 8.3 Hz, 4H), 7.17(d, J = 16 Hz, 2H), 7.13 (d, J = 16 Hz, 2H), 6.91 (d, J = 8.3 Hz, 4H), 4.00 (t, J = 5.7 Hz, 4H), 3.82 (s, 6H), 3.76 (t, J = 5.7 Hz, 4H), 3.55 (m, 4H), 3.45 (m, 4H), 3.32 (s, 6 H). ^{13}C NMR (75.75 MHz, $CDCl_3$) δ ppm 163.11, 159.78, 148.451, 140.62, 132.55, 130.45, 129.75, 128.12, 126.51, 126.45, 125.66, 114.26, 109.73, 71.85, 70.517, 68.98, 59.07, 55.37, 44.23. HRMS m/z calcd for $C_{46}H_{48}N_2O_8$ 756.34107, found 756.34155.

Peptide Synthesis and Bioconjugation. Tat (44-61) sequence was synthesized by solid-phase peptide (SPPS) chemistry using the Fmoc procedure with an automatic peptide synthesizer (ABI 433A, Appelar, France) as previously described.[17] Briefly, 207 mg of Fmoc-Leu-Wang resin LL was used (substitution 0.3 mmol/g) at 0.1 mmol scale and all amino acids were coupled through HBTU/HOBt as coupling agents. Deprotection of the Nα Fmoc protecting group was obtained with a 6 min piperidine treatment followed by UV at 301 nm. The peptide was ended by a β-alanine derivative used as a spacer between peptide and fluorescent probe. Then, two batches of 0.006 mmol resin were isolated and incubated in 400 μL of NMP containing 0.028 mmol (4 equiv of **10**, 20 mg) or **5** (20 mg), 6 μL HBTU 0.45 M, and 24 μL of DIEA 2 M for 24 h at room temperature. After filtration and MeOH washings, the peptidyl-resin was cleaved for 2 h in a trifluoroacetic acid (TFA) solution containing phenol (2%, w/v), tri(isopropyl)-silane (5%, v/v), and H_2O (2.5%, v/v). After ether precipitation, peptides were purified by reverse-phase high-performance liquid chromatography on a C8 column (uptisphere 300 Å, 5 μm; 250 × 10, Interchim, France). Molecular masses were obtained by ion spray mass spectrometry, m/z found for Tat(44-61)-**5** [$MH^{+\bullet}$] 2977.59 (calcd 2976.59) and Tat(44-61)-**10** [$MH^{+\bullet}$] 2974,65 (calcd 2970.64). The purity of these two peptides was estimated >95% by HPLC. The yields of the fluorescently tagged peptides were in the 30% range for Tat(44-61)-**5** and Tat(44-61)-**10**. Prior to use, peptides were dissolved in distilled water, aliquoted, and stored at −20 °C.

Two-Photon Absorption Properties. The TPA cross-section spectra were obtained by up-conversion fluorescence using a Ti:sapphire femtosecond laser in the range 750−900

Scheme 1. Preparation of Peripherally Substituted Acidic Fluorophore 5[a]

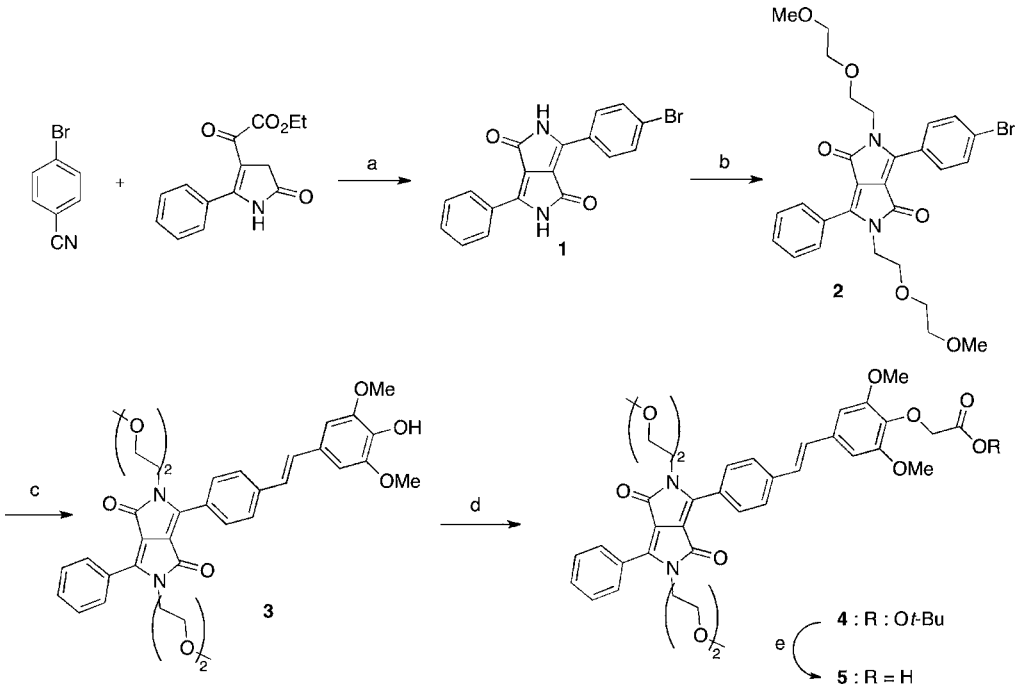

[a]Reagents and yields: (a) *tert*-amyl alcohol, Na, 70%. (b) NMP, *tert*-BuOK, 1-bromo-2-(2-methoxyethoxy)ethane, 36%. (c) $Pd(OAc)_2$, TOP, DMF/Et_3N, 4-(*tert*-butyldimethylsilanyloxy)-3,5-dimethoxystyrene, 76%. (d) DMF, K_2CO_3, *tert*-butyl bromoacetate, 30%. (e) CH_2Cl_2, TFA, 97%.

nm as previously described.[18] The excitation beam is collimated over the cell length (10 mm). The fluorescence, collected at 90° of the excitation beam, was focused into an optical fiber connected to a spectrometer. The incident beam intensity was adjusted to ensure an intensity-squared dependence of the fluorescence over the whole spectral range. Calibration of the spectra was performed by comparison with Rhodamine B two-photon absorption spectrum.[20]

Spectroscopic Measurements. All UV−vis absorption spectra were recorded on a Cary 400 spectrophotometer in a dual beam mode using a matched pair of 1 cm × 1 cm quartz cells. Pure solvent was used as reference. Values of the molar extinction coefficients, ε_{max}, of the compounds of interest were obtained as the average of at least five independent measurements with absorbance in the range 0.5−1. Fluorescence emission and excitation spectra were obtained with optically dilute solutions (abs < 0.15) in 1 cm × 1 cm cells using a Fluorolog (Jobin-Yvon) spectrofluorometer. Fluorescence quantum yields were measured by the relative method, using Rhodamine B in methanol[19] as the reference. In these measurements, the slit widths were adjusted so that the spectral bandwidth of the absorption and emission instruments were identical at 1.0 nm, and the absorbance of the sample and the reference were chosen so they were in the 0.1−0.15 range and nearly identical at the same excitation wavelength. Emission quantum yields were then calculated according to the method described by Crosby and Demas, taking into account the differences between the refractive indices of the sample and reference solutions.[20]

Two-Photon Imaging. Two-photon microscopy was performed on a home-built setup.[21] Two-photon excitation (TPE) is provided by a Tsunami Ti:sapphire laser pumped with a Millennia V solid-state laser (Spectra-Physics, Mountain View, CA). Pulses of ∼100 fs are produced with a 80-MHz frequency at 760 nm. After a beam expander, the infrared light is focused into the sample by a water immersion Olympus objective (60×, NA = 1.2) mounted on an Olympus IX70 inverted microscope. The back aperture of the objective was slightly overfilled, creating a diffraction-limited focal spot. Samples were placed in an eight-well Lab-Tek chambered cover glass (Nalge Nunc International, Rochester, NY) positioned in the *x* and *y* directions by a motorized stage (Märzhäuser, Germany). The fluorescence from the samples was collected through the same objective and directed by a COWL750 dichroic mirror (Coherent, Orsay, France) toward a 50-μm diameter optical fiber coupled to an avalanche photodiode (SPCM 200 FC, EG&G, Canada). The residual infrared light was rejected by a BG39 Filter (Coherent). The imaging system was based on the use of two galvo mirrors (model 6210, Cambridge Technology), in the so-called descanned detection mode. The two mirrors were used to deflect the beam along the *x*-axis and *y*-axis, respectively. Each axis was driven by a closed loop power amplifier, and the position of the mirrors was controlled through two ADC electronic boards (PCI6711, National Instruments). The photons were counted using a counter/timer board (PCI6602, National Instruments), synchronized with the scan of the galvo mirrors. Nominally, one picture is 512 × 512 in size, and the dwelling time for each pixel is 4 μs (about 1 s per scan).

RESULTS AND DISCUSSION

Synthesis of New Fluorescent Two-Photon Probes and Bioconjugation. We explored two ways to attach a biomolecule on a DPP-centered fluorophore: one for which the biomolecule is attached on the periphery of the fluorophore (**5**) and a second one for which the bioconjugation occurs on the central DPP core (**10**). The key intermediate for the synthesis of **5** is a dissymmetrical DPP core substituted by a phenyl ring on one side and by a 4-bromophenyl moiety on the other side

dx.doi.org/10.1021/bc300623q | *Bioconjugate Chem.* 2013, 24, 942−950

Scheme 2. Molecular Structures of Tat (44-51) Bioconjugates 5-βAla−Tat and 10-βAla−Tat

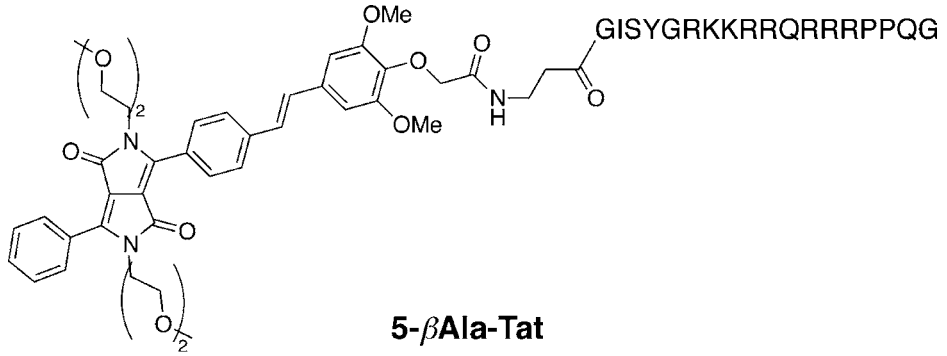

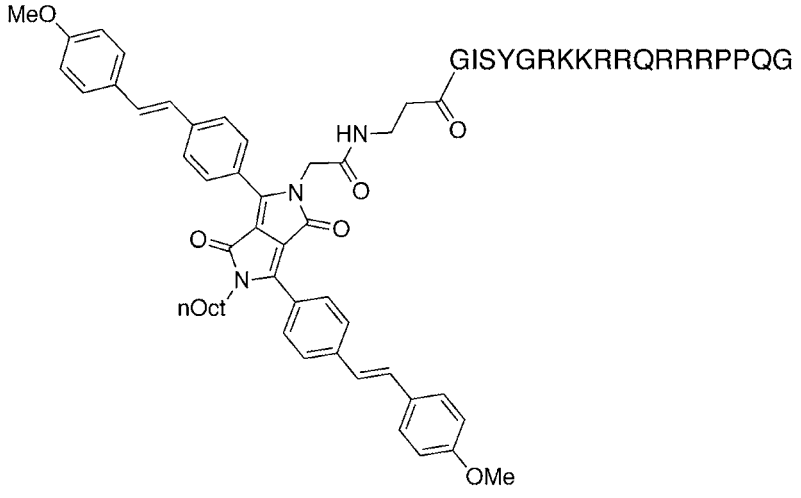

Scheme 3. Preparation of Centrally Substituted Acidic Fluorophore 10[a]

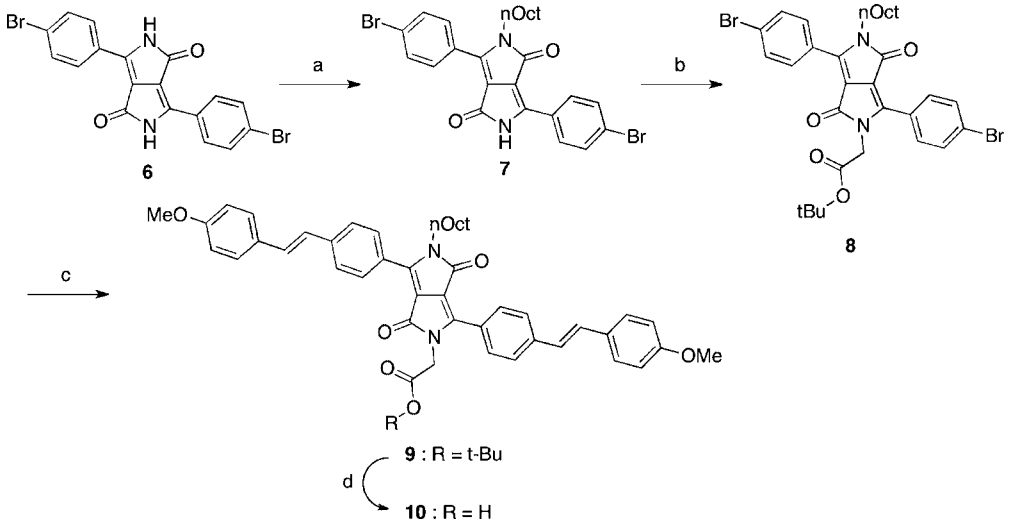

[a]Reagents and yields: (a) NMP, *t*-BuOK, 1-bromooctane, 36%. (b) NMP, *t*-BuOK, *tert*-butyl bromoacetate, 47%. (c) $Pd(OAc)_2$, TOP, DMF/Et_3N, 4-vinylanisole, 86% DMF. (d) CH_2Cl_2, TFA, 85%.

(**1**), allowing on this side classical palladium cross-coupling further reactions (Scheme 1).

Usually DPP cores are obtained by a cascade reaction between di-isopropyl succinate and 2 equiv of aromatic nitrile molecules.[14] For the preparation of the dissymmetrical substituted DPP, the reaction proceeds in two steps. First, a pyrrolinone ester was isolated by reaction of ethyl benzoylacetate and methyl chloroacetate in moderate basic medium,

dx.doi.org/10.1021/bc300623q | *Bioconjugate Chem.* 2013, 24, 942−950

followed by reaction with an ammonium salt and then reaction with an aromatic nitrile. Second, this last compound reacts with another aromatic nitrile in strong basic conditions to give **1**.[16] As for all non-alkylated DPP molecules, **1** is highly insoluble in classical solvents, and to induce a good solubility in water, we introduced short oligo(ethylene glycol) chains on each nitrogen atom as described previously, leading to the monobromo DPP derivative **2**.[14] Then a Heck coupling between **2** and 4-(*tert*-butyldimethylsilanyloxy)-3,5-dimethoxystyrene followed by in situ deprotection of the silylated group gave compound **3** in good yield. The reactive moiety was then introduced on the free phenolic group by reaction with *tert*-butyl bromoacetate. The ester bond was then cleaved to give the acidic function, which can be used directly in solid-phase peptide synthesis. The bioconjugation was performed directly with Tat peptide on solid-phase synthesis support, and the peptide−fluorophore conjugate was cleaved by TFA treatment. The bioconjugate Tat derivative was then purified by HPLC and characterized by LC−MS. A β-amino acid in the N-terminus of the peptide was introduced to increase its stability (Scheme 2).[22]

The preparation of the central core functionalized DPP-based fluorophore uses symmetrical bis-4-bromophenyl substituted DPP **6** (Scheme 3). The substitution of hydrogen atoms of the DPP core proceeds in two steps. The first was the introduction of a single octyl group on the core (**7**). The remaining hydrogen atom was then substituted with *tert*-butyl bromoacetate to give the key synthon **8** as previously described.[23] This last was then submitted to a bis-Heck coupling with 4-vinylanisole to give **9** in very good yield. The acidic fluorophore **10** was then obtained by TFA treatment. The Tat conjugate was obtained using the same method as for **5** (Scheme 2).

Photophysical Properties. The photophysical properties of fluorophore **4** and **9** were investigated by UV−vis and fluorescence spectroscopy, and the corresponding spectra are shown in Figure 2. The absorbance of these two functionalized dyes are very similar to the ones of model compounds. Table 1 summarizes their photophysical parameters. As previously reported, the nature of the electron-donating group of the phenyl ring in the periphery of the DPP core does not induce drastic changes in the one-photon photophysical properties.[14] Fluorophores **4** and **9** show a strong absorption around 500 nm and bright orange fluorescence around 600 nm (Table 1). The removal of the vinylanisole group on one side of the fluorophore induces a blue shift of 747 cm^{-1} in the absorbance spectrum and of 643 cm^{-1} in the fluorescence spectrum due of the diminution of the conjugated system length combined with the loss of one of the electron-donating group (methoxy). Interestingly, the introduction of the acidic reactive moiety useful for bioconjugation does not affect significantly the photophysical properties of these dyes, as it is not in a conjugated position that could affect the polarizability compared to that of the parent dyes (2,5-bis(2-(2-methoxyethoxy)ethyl)-3,6-bis(4-((*E*)-4-methoxystyryl)phenyl)-pyrrolo[3,4-*c*]pyrrole-,4(2*H*,5*H*)-dione (**11**) and 2,5-bis(2-(2-methoxyethoxy)ethyl)-3,6-bis(4-((*E*)-3,4,5-tris(2-(2-(2-methoxyethoxy)ethoxy)ethoxy)styryl)phenyl)pyrrolo[3,4-*c*]-pyrrole-1,4(2*H*,5*H*)-dione (**12**) described previously[14] (Figure 3).

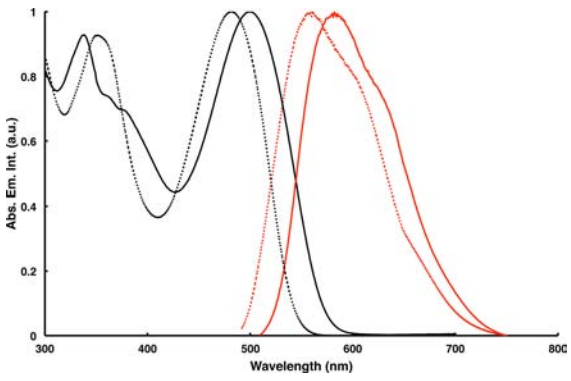

Figure 2. Absorption (black) and emission (red) spectra of **4** (dashed) and **9** (plain) in dichloromethane.

The absorption spectra of the two conjugates (Figure 4) are very similar to those of the parent dyes, indicating that the conjugation does not alter the absorption properties of the two dyes (128 and 40 cm^{-1} red shift for **5** and **10**, respectively). In contrast, for the emission spectra, we can notice a strong blue shift of 2055 and 2929 cm^{-1} for **5** and **10**, respectively, with a bright yellow emission (550−600 nm) that can be attributed to a better solubilization in aqueous media due to the hydrophilic Tat peptide. Combined with a small effect on the absorption spectra, the Stokes shifts of the two dyes are greatly reduced upon bioconjugation. This diminution of stokes shift, which should be problematic in confocal or epifluorescence microscopy (as the excitation wavelength would be close to the emission wavelength) is indeed not problematic in TPEM because the excitation wavelength used (in the IR region) is well separated from the emission.

The two-photon properties of fluorophores **4** and **9** were investigated experimentally by the two-photon fluorescence method. Their two-photon excitation spectra are shown in Figure 5.

The shapes of the spectra of these two dyes are similar with maxima in the 820−840 nm range, but the two-photon absorption cross-section of the functionalized divinylanisole dye **9** is about twice the one of the dissymmetric molecule **4**. Two-photon absorption cross-section of **9** is in the same range as the one obtained for the reference molecule **11**. Two-photon absorption maxima of these molecules occur in the 820 nm region, which is red-shifted compared to other bioconjugatable two-photon dyes described in the literature for which the maxima are lower than 720 nm, with two-photon absorption

Table 1. Photophysical Properties of Dyes 4 and 9 and the Two Model Compounds 11 and 12 in Dichloromethane and Water (in Brackets)

dye	λ_{max} abs (nm)	ε (M^{-1} cm^{-1})	λ_{max} em (nm)	Φ (%)	σ_2 (GM) at 800 nm
4	482 (501)	15000 (16000)	561 (586)	34	350
9	500 (507)	30000 (12000)	582 (619)	68	700
11	503 (501)	35000 (20000)	580 (597)	70 (5)	750
12	501 (510)	23700 (4900)	581 (572)	52 (2)	750

dx.doi.org/10.1021/bc300623q | *Bioconjugate Chem.* 2013, 24, 942−950

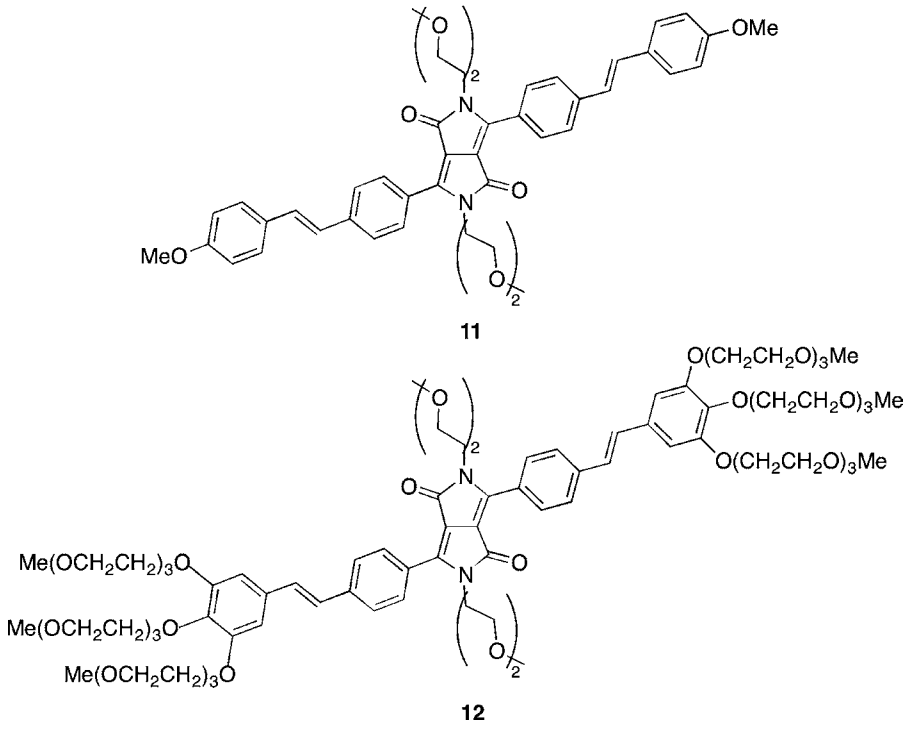

Figure 3. Molecular formulas of parent fluorophores **11** and **12**.

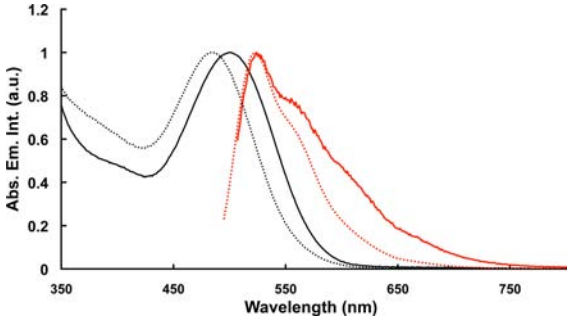

Figure 4. Absorption (black) and emission (red) spectra of **5-βAla–Tat** (dashed) and **10-βAla–Tat** (plain) conjugates in water.

cross-section in the same range.[9,12] Combined with the difference in two-photon induced fluorescence color (yellow for **9**, blue[9] and green[12] for bioconjugatable fluorene derivatives), these dyes are good candidates for fully two-photon optimized multicolor labeling.

Two-Photon Imaging. Fluorescently tagged Tat peptides **5-βAla–Tat** and **10-βAla–Tat** were used in two-photon excited microscopy on HeLa cell cultures. Figures 6 and 7 represent characteristic phenotypes observed on the whole cell culture.

First, to evaluate the fluorescent potency of the bioconjugate **5-βAla–Tat** in cellular context, several trials with increased concentrations were carried out. Thus 0.5, 1, and 10 μM

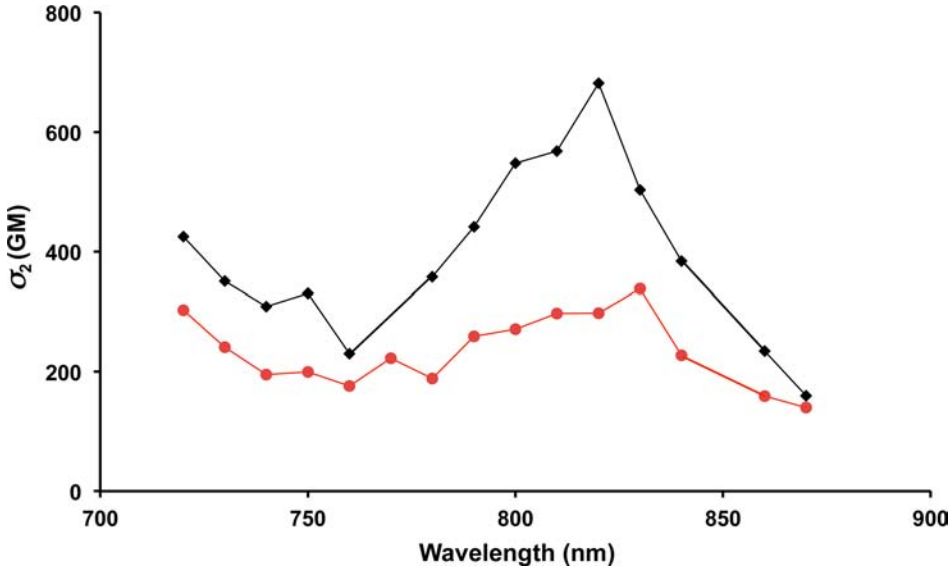

Figure 5. Two-photon excitation spectra of **4** (red) and **9** (black) in methylene chloride.

dx.doi.org/10.1021/bc300623q | *Bioconjugate Chem.* 2013, 24, 942–950

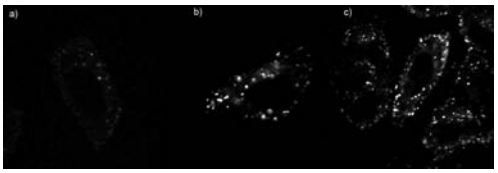

Figure 6. Two-photon excited microscopy on HeLa cells incubated in 0.5 (a), 1 (b), and 10 μM (c) solutions of **5-βAla−Tat**, after 1 h incubation (λ_{ex} 800 nm, average laser power <5 mW).

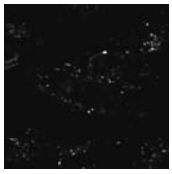

Figure 7. Two-photon excited microscopy on HeLa cells incubated in 1 μM solution of **10-βAla−Tat** after 1 h of incubation (λ_{ex} = 800 nm, average laser power <1 mW).

solutions of **5-βAla−Tat** were incubated for 1 h with preseeded adherent HeLa cells. Then, cells were quickly washed with trypsin to remove the background and left for 1−4 h before image analysis. All experiments were performed in glass-bottom dishes, allowing the live cells to be viewed by microscopy in buffered solution, avoiding the possible artifacts in peptide distribution that could occur with fixed cells.[24] At low concentration (0.5 μM, Figure 6a), a punctuate cytoplasmic distribution of the peptide was observed. This pattern of distribution was also observed when the concentration of **5-βAla−Tat** was raised up to 10 μM (Figure 6b,c). A detailed analysis of two-photon *z*-stack images revealed that most of the dots were inside the cell. Interestingly, at high concentration (1 and 10 μM) of **5-βAla−Tat** additional diffuse fluorescence signal was observed in the cytoplasm, likely resulting from Tat diffusing throughout the cell after its release from endocytic vesicles. Finally, no staining was observed in the nucleus with **5-βAla−Tat**, suggesting that the probe **4** did not induce artifactual distribution of the peptide as compared to its fluorescein counterpart.[25] Thus, dye **4** does not seem to interfere with the cellular endocytosic uptake described for Tat derivatives,[26] emphasizing the use of this two-photon probe for cellular imaging. **10-βAla−Tat** was then used at low concentration (1 μM) on HeLa cells culture and showed remarkable ability to stain cells and to allow TPEM images in the sub milliwatt range due to its better two-photon absorption cross-section, while similar images needed 5 mW laser power for **5-βAla−Tat** (Figure 7).

CONCLUSION

We described here the conception, synthesis, characterization, and uses of two new DPP-based bioconjugatable fluorescent dyes for two-photon excited microscopy. They were successfully coupled to a synthetic Tat-derived peptide as two-photon fluorescent tag for living cell microscopy with low power excitation (in the sub-milliwatt range for **10**). The versatility of the bioconjugation and the efficiency of these two-photon sensitive yellow fluorescent dyes make them very good candidates for multicolor labeling of biomolecules for two-photon excited microscopy in association with other optimized two-photon bioconjugatable fluorophores (such as blue[9] and green[12] fluorescent ones).

AUTHOR INFORMATION

Corresponding Author

*E-mail: frederic.bolze@unistra.fr.

Notes

The authors declare no competing financial interest.

ACKNOWLEDGMENTS

Dr. Ludovic Richert and Prof. Yves Mély are acknowledged for two-photon excited microscopy. Dr. Zeinab Darwich is acknowledged for providing HeLa cell cultures. H.F. thanks the "Ministère de l'Enseignement Supérieur et de la Recherche" (MESR) for a fellowship. GDR 2588 is also gratefully acknowledged for discussions.

REFERENCES

(1) Helmchen, F., and Denk, W. (2005) Deep tissue two-photon microscopy. *Nat. Methods 2*, 932−940.

(2) Larson, A. M. (2011) Multiphoton microscopy. *Nat. Photonics 5*, Advertising feature.

(3) Soeller, C., and Cannell, M. B. (1999) Two-photon microscopy: Imaging in scattering samples and three-dimensionally resolved flash photolysis. *Microsc. Res. Tech. 47*, 182−195.

(4) Warther, D., Gug, S., Specht, A., Bolze, F., Nicoud, J.-F., Mourot, A., and Goeldner, M. (2010) Two-photon uncaging: new prospects in neuroscience and cellular biology. *Bioorg. Med. Chem. 18*, 7753−7758.

(5) Squirrell, J. M., Wokosin, D. L., White, J. G., and Bavister, B. D. (1999) Long-term two-photon fluorescence imaging of mammalian embryos without compromising viability. *Nat. Biotechnol. 17*, 763−767.

(6) König, K. (2000) Multiphoton microscopy in life sciences. *J. Microsc. 200*, 83−104.

(7) Pawlicki, M., Collins, H. A., Denning, R. G., and Anderson, H. L. (2009) Two-photon absorption and the design of two-photon dyes. *Angew. Chem., Int. Ed. 48*, 3244−3266.

(8) Larson, D. R., Zipfel, W. R., Williams, R. M., Clark, S. W., Bruchez, M. P., Wise, F. W., and Webb, W. W. (2003) Water-soluble quantum dots for multiphoton fluorescence imaging in vivo. *Science 300*, 1434−1436.

(9) Hayek, A., Ercelen, S., Zhang, X., Bolze, F., Nicoud, J.-F., Schaub, E., Baldeck, P. L., and Mély, Y. (2007) Conjugation of a new two-photon fluorophore to poly(ethylenimine) for gene delivery imaging. *Bioconjugate Chem. 18*, 844−851.

(10) Bolze, F., Niehl, A., Heinlein, M., Mjdasiri, N., Rehspringer, J.-L., Schaeffer, N., Didier, P., Arntz, Y., Mély, Y., Gug, S., Specht, A., Goeldner, M., and Nicoud, J.-F. (2010) Two-photon excitation in life sciences: From observation to action. *Nonlinear Opt., Quantum Opt. 40*, 253−265.

(11) Morales, A. R., Yanez, C. O., Schafer-Hales, K. J., Marcus, A. I., and Belfield, K. D. (2009) Biomolecule labeling and imaging with a new fluorenyl two-photon fluorescent probe. *Bioconjugate Chem. 20*, 1992−2000.

(12) Yao, S., and Belfield, K. D. (2012) Two-photon fluorescent probes for bioimaging. *Eur. J. Org. Chem. 17*, 3199−3217.

(13) Iqbal, A., and Cassar, L. (Ciba-Geigy) (1982) 1,4-Diketopyrrolo[3,4-*c*]pyrrole pigments. Patent EP 98808 .

(14) Ftouni, H., Bolze, F., and Nicoud, J.-F. (2013) Water-soluble diketopyrrolopyrrole derivatives for two-photon excited fluorescence microscopy. *Dyes Pigments 97*, 77−83.

(15) Vyňuchal, J., Luňák, S., Jr, Hatlapatková, A., Hrdina, R., Lycka, A., Havel, L. Å., Vyňuchalová, K., and Jirásko, R. (2008) The synthesis, absorption, fluorescence and photoisomerisation of 2-aryl-4-arylmethylidene-pyrroline-5-ones. *Dyes Pigments 77*, 266−276.

(16) Luňák, S., Jr, Vyňuchal, J., Vala, M., Havel, L., and Hrdina, R. (2009) The synthesis, absorption and fluorescence of polar diketo-pyrrolo-pyrroles. *Dyes Pigments 82*, 102−108.

(17) Greiner, V. J., Shvadchak, V., Fritz, J., Arntz, Y., Didier, P., Frisch, B., Boudier, C., Mély, I., and de Rocquigny, H. (2011)

Characterization of the mechanisms of HIV-1 Vpr(52−96) internalization in cells. *Biochimie 93*, 1647−1658.
(18) Xu, C., Williams, R. M., Zipfel, W., and Webb, W. W. (1996) Multiphoton excitation cross-sections of molecular fluorophores. *Bioimaging 4*, 198−207.
(19) Xu, C., and Webb, W. W. (1996) Measurement of two-photon excitation cross-sections of molecular fluorophores with data from 690 to 1050 nm. *J. Opt. Soc. Am. B 13*, 481−491.
(20) Crosby, G. A., and Demas, J. N. (1971) Measurement of photoluminescence quantum yields. *J. Phys. Chem. 75*, 991−1024.
(21) Nicoud, J.-F., Bolze, F., Sun, X.-H., Hayek, A., and Baldeck, P. L. (2011) Boron-containing two-photon-absorbing chromophores. 3. (1) One-and two-photon photophysical properties of p-carborane-containing fluorescent bioprobes. *Inorg. Chem. 50*, 4272−4278.
(22) Henschen, A., and Edman, P. (1972) Large scale preparation of S-carboxymethylated chains of human fibrin and fibrinogen and the occurrence of chain variants. *Biochim. Biophys. Acta 263*, 351−367.
(23) Guo, E. Q., Ren, P. H., Zhang, Y. L., Zhang, H. C., and Yang, W. J. (2009) Diphenylamine end-capped 1,4-diketo-3,6-diphenylpyrrolo-[3,4-*c*]pyrrole (DPP) derivatives with large two-photon absorption cross-sections and strong two-photon excitation red fluorescence. *Chem. Commun.*, 5859−5861.
(24) Richard, J. P., Melikov, K., Vives, E., Ramos, C., Verbeure, B., Gait, M. J., Chernomordik, L. V., and Lebleu, B. (2003) Cell-penetrating peptides. A reevaluation of the mechanism of cellular uptake. *J. Biol. Chem. 278*, 585−590.
(25) Vives, E., Richard, J. P., Rispal, C., and Lebleu, B. (2003) TAT peptide internalization: seeking the mechanism of entry. *Curr. Protein Pept. Sci. 4*, 125−132.
(26) Brooks, H., Lebleu, B., and Vives, E. (2005) Tat peptide-mediated cellular delivery: back to basics. *Adv. Drug Delivery Rev. 57*, 559−577.